Published by :
http://www.ijert.org

International Journal of Engineering Research & Technology (IJERT)
ISSN: 2278-0181
Vol. 11 Issue 04, April-2022

Experimental Investigation of a Non Integer Control for a Micro-Grid Integrated Battery Storage System using Dual Active Bridge

Alsharef Mohammad
Department of Electrical Engineering, College of Engineering,
TAIF University KSA,

***Abstract*—This paper addresses the voltage regulation problem of a micro-grid integrated battery storage system driven by single phase dual active bridge (DAB) using fractional order proportional, integral derivative (FOPID) control system. The fractional operators are approximated using infinite impulse response (IIR) filter and the corresponding FOPID control system is realized using TI Launchpad (TMS320F28379D) for a low power bi-directional converter using rapid prototyping concepts from MATLAB/Simulink environment. The controller is tested with variable reference command and the results are compared experimentally with integer order PID control system. From the presented experimental results, it is obvious that I comparison to the classical proportional, integral derivative (PID) controller, the proposed method ensures fast transient response and lowest steady state error.**

Keywords—DC microgrid, dual active bridge, PID control, fractional order control.

I. INTRODUCTION

Due to rise in environmental pollution, human community is compelled to explore clean and sustainable energy resources and infrastructure, therefore inclination of modern world for energy utilization is more towards clean power generation [1]. However, the unpredictable nature of these renewable sources requires stable integration of such sources into the micro-grid, which is very complex. The small-scale micro-grid consists of different generation sources and all these are connected to the common the common bus.

Generally there are two types of converters i.e. isolated and non-isolated type converters. The isolated converters are mainly used for bidirectional power flow [2]. DAB converter is the most promising topology in isolated converters allowing bidirectional power flow, soft switching operation and high power density. Due to these advantages, various applications of DAB are distributed power systems, renewable energy systems, and hybrid / electric vehicles and so on [3-7].

Moreover, to reduce switching losses, Single phase shift (SPS) modulation technique is the most commonly used technique. In SPS technique, phase shifts ϕ is inserted between the primary and secondary side bridges of the transformer. Other modulation technique such as enhanced phase shift (EPS), double and triple phase shift (DPS&TPS) are also reported to minimize high circulating current [8-9]. In DPS There are two degrees of freedom, namely phase shift ϕ1and ϕ2 to adjust the control of the power flow. ϕ1is introduced between the complementary switches of the primary side bridge whereas, the outer phase shift ϕ2 is incorporated between the two bridges of the DAB. Furthermore, triple phase shift modulation technique implements three-degree control variable [10]. However, these modulation techniques have their own limitations due to their higher degrees of complexities.

Stable regulation of output voltage requires close loop control techniques. Several control strategies have been proposed, including linear and non-linear control techniques. Linear controllers such as single loop or dual loop PID are easy to implement. However, variation in circuit parameters and model uncertainties can degrade the converter performance. Fixed gain PI controller is reported in [11-12] and Artificial Neural Network (ANN) based control is proposed in [13]. Apart from linear, nonlinear control techniques show encouraging performance under circumstance of variable source or load. However, nonlinear controllers are complex and require more computational time for its implementation [14-16]. This paper proposes fractional order PID control method for voltage loop of the secondary side bridge of the DAB topology. The organization of the paper is detailed as following. Section II represents Notation; Section III discusses problem formulation. Section IV presents the results and discussion. Conclusion is made in section V

II. PROBLEM STATEMENT

A. Dual active bridge configuration

Block diagram representations of a DC micro-grid and DAB converters are shown in figure 1a and figure 1b respectively. As shown in the diagram, two H-bridges are integrated using high frequency transformer. Each H-bridge comprises of four switching devices, a dc capacitors and leakage inductor Ls is connected with secondary of high frequency transformer. Square voltage wave forms are obtained by switching the bridges H1 and H2 by using complementary constant pulse width modulating signal (PWM) with 50% duty cycle. Bidirectional power flow is possible by adjusting the parameter ϕ of the output voltages V1 and V2 of H-bridges respectively

International Journal of Engineering Research & Technology (IJERT)
ISSN: 2278-0181
Vol. 11 Issue 04, April-2022

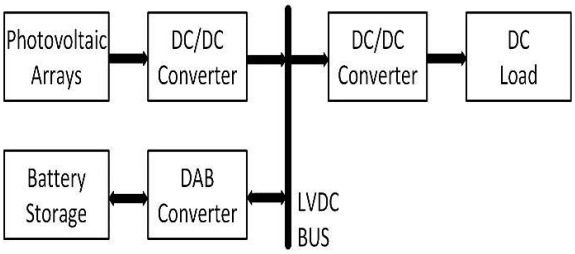

(a)

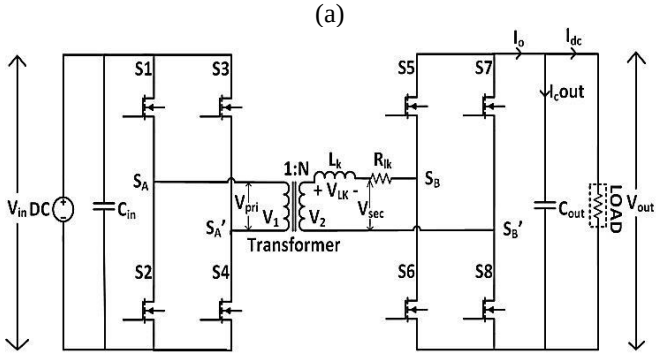

(b)

Figure 1 (a) DC mico-grid (b) Configuration of bidirectional dual active bridge converter

In SPS, the output power can be expressed by the following expression.

$$P_o = \frac{nV_{in}V_{out}}{2\pi^2 f_s L_k}\emptyset(\pi - \emptyset) \quad \emptyset \in \left[-\frac{\pi}{2}, +\frac{\pi}{2}\right] \qquad (1)$$

Where fs is the frequency of switching and n represents the transformer turn ratio. Capacitors of 100 µ F and 330 µ F are connected at both ends to smooth the output voltage. Referring to [1], and based on 1st harmonic of the Fourier series the state model of a DAB converter is expressed as follows:

$$\dot{X} = A(x) + B(x)U \qquad (2)$$

Where the terms *A(x)* and *B(x)* are expressed as follows

$$\begin{cases} A(x) = \dfrac{-8}{C_{out}\pi^2} \displaystyle\sum_{n=1,3,5,..}^{\infty} \frac{\cos(\varphi_z(n))}{n^2|Z(n)|} V_{out} \\ B(x) = \dfrac{8}{C_{out}\pi^2} \displaystyle\sum_{n=1,3,5,..}^{\infty} \frac{1}{n^2|Z(n)|} NV_{in} \end{cases} \qquad (3)$$

,

Where $|Z(n)|$ represents the impedance of the two bridges, C_{out} represents output capacitance and $\varphi_z(n)$ represents the phase difference of the modulating signals between the two bridges of the DAB converter.

B. *Classical proportional integral (PI) control*

The expression for a classical PI controller is expressed as follows:

$$u = k_p e(t) + k_i \int e(t)dt + k_d e(t) \qquad (4)$$

where k_p, k_i, k_d refer to the control system gains. The error term is defined as follows: $e(t) = x(t) - x_d(t)$. where $x(t)$ is the system output voltage and $x_d(t)$ is the reference signal. In addition, in real scenarios, reference signal is variable, therefore the selection of k_p and k_i has to be done carefully to increase the tracking accuracy of the voltage loop. In addition, SPS modulation technique is used to generate the drive signal. Since a digital processor is used in the experimentation, therefore high frequency phase shifted PWM signals are generated to drive the bidirectional DAB converter. However; due to the incomplete knowledge of the model parameters and ignorance of high order dynamics in the DAB model [1], selection of the optimal parameters of the classical PI controller is a challenging task. Therefore in the subsection discussed below, a non-integer PI controller is introduced with high degree of freedom to adjust system performance.

C. *Fractional order control*

In this subsection, fractional order control system is introduced. Fractional order controllers offer several advantages over the conventional methods such as high degree of freedom, robustness to noise and robustness. A general representation of a non-integer PID controller is represented in figure 2.

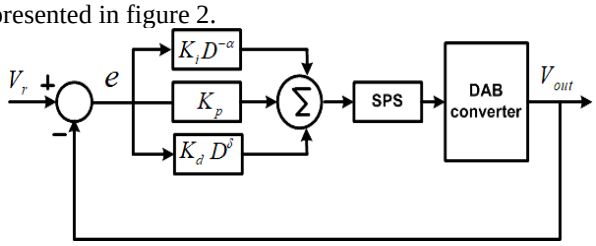

Figure 2 Fractional order PID control

As shown in figure 2, a fractional order PID controller has a total of five degrees of freedom that includes K_p , K_i , K_d , $D^{-\alpha}$ and D^{δ} . Where α and δ represent the fractional orders of integration and derivative terms.

Before expressing a fractional order PID control method, we introduce some basic fractional order definitions.

Definition 1:

Fractional operator is defined as given in Eq. 3 [17].

$$aD_t{}^{\alpha} \cong \begin{cases} \frac{d^{\alpha}}{dt^{\alpha}}, R(\alpha) > 0 \\ 1, R(\alpha) = 0 \\ \int_a^t d\tau^{\alpha}, R(\alpha) < 0 \end{cases} \qquad (5)$$

Where R (α) is set of real numbers, based on (5), the definition of fractional operator is characterized into following three categories [17].

Definition 2:

The Riemann–Liouville definition is given in Eq. 6 and 7. [18].

$$aD_t{}^{\alpha}x(t) = \frac{d^{\alpha}}{dt^{\alpha}}x(t) = \frac{1}{\Gamma(m-\alpha)dt^m}\int \frac{x(\tau)}{(t-\tau)^{\alpha-m+1}}d\tau \qquad (6)$$

International Journal of Engineering Research & Technology (IJERT)
ISSN: 2278-0181
Vol. 11 Issue 04, April-2022

$$aD_t^{-\alpha}x(t) = I^{\alpha}x(t) = \frac{1}{\Gamma(\alpha)}\int \frac{x(\tau)}{x(t-\tau)^{1-\alpha}}d\tau \quad (7)$$

Here $m-1 < \alpha < m$ and **G",** represents the Gama function.

Definition 3: The Caputo definition is given in Eq. 6 [18].

$$aD_t^{\alpha} = \begin{cases} \frac{1}{\Gamma(n-\alpha)}\int_{\alpha}^{t} \frac{x^n(\tau)}{(t-\tau)^{\alpha-n+1}}d\tau (n-1 \le \alpha < n) \\ \frac{d^m}{dt^n}x(t)(\alpha = n) \end{cases} \quad (8)$$

Definition 4: For a givenα, the GL definition is expressed as following [18],

$$ {}_a^{GL}D_t^{\alpha}x(t) = \lim_{h\to 0}\frac{1}{h^{\alpha}}\sum_{j=0}^{[(t-\alpha)/h]}(-1)^j\binom{\alpha}{j}x(t-jh)$$

$$\binom{\alpha}{j} = \frac{\Gamma(\alpha+1)}{\Gamma(j+1)\Gamma(\alpha-j+1)} \quad (9)$$

From (9), the Gama function and time step are represented by Γ and h respectively. Based on above definitions, the fractional order PID controller is defined as follows.

$$u(t) = K_p e(t) + K_i D_t^{-\alpha}e(t) + K_d D_t^{\delta}e(t) \quad (10)$$

Therefore, the fractional control system depends on the adjustment of parameters i.e.$k = K_p, K_i, K_d$ and the fractional orders α, δ.

D. Implementation of fractional operator

The fractional controllers are becoming popular because of its robustness and high flexibilities in design. However, the real time implementations of FOPI controller are far different from its integer counterpart as it involves the fractional integrator and differentiator, which has high memory requirements. To implement the FOPI controller, proper approximation is required for the integrator and differentiators. In this paper, Oustaloup filter is used for the approximation of non-integer integrator and differentiator. The filter provides the continuous-domain values of poles and zeros that are converted into z-domain and finally using IIR filter the practical implementations are carried out. Rest of the process is carried out according to the steps as shown in Figure 3.

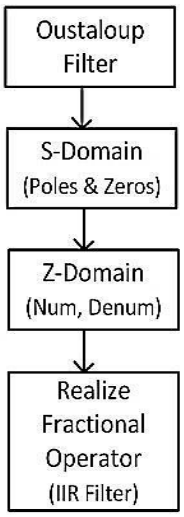

Figure 3 Steps for practical implementation of fractional operator

III. EXPERIMENTAL SETUP

To implement the FOPI controller, a scaled down laboratory test bench of 150 watts power rating is developed as shown in Fig. 4. A 12 V DC power supply is connected with the primary bridge H_1 and 24 V battery bank is connected with secondary bridge H_2. The proposed control scheme is implemented using a Texas Instrument Launchpad control card TMS320F28379D with a sampling time of 1e-5 seconds. The details of circuit parameters for the experimental setup are shown in table I and controller parameters are shown in table II.

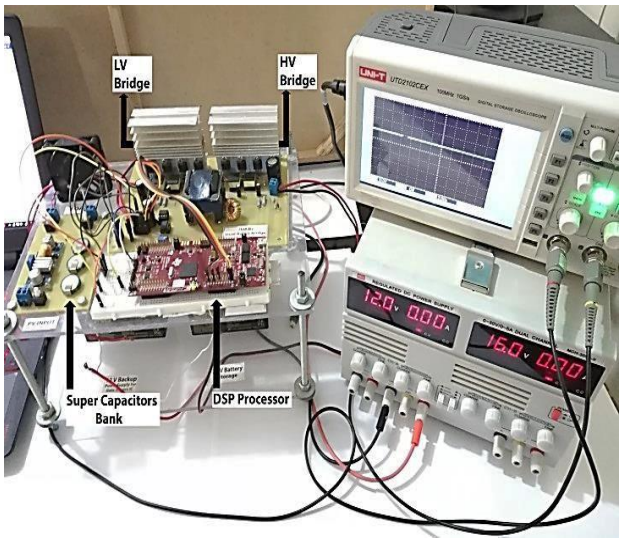

Figure 4 Experimental Setup of DAB converter testing

Table I: system Parameters

Symbol	QUANTITY	Values
P	Power rating	50W
Vin	Voltage input	12 V
Vo	Voltage output	24 V
C_{in}, C_{out}	Capacitance	100µF, 330µF
N	Transformer Turn	1:2
L_k	Ratio	50µH
R	Equivalent inductor	100 Ah
	Load	

International Journal of Engineering Research & Technology (IJERT)
ISSN: 2278-0181
Vol. 11 Issue 04, April-2022

Table II. Control System Parameters

Controll	Parameters	Value
PI	Kp	2.5
	Ki	2.5
FOPI	α	-0.99
	δ	0.0

Moreover the discrete Simulink model of the proposed FO-PI and integer order PI controllers are programmed using real-time workshop and embedded coders and using rapid prototyping the obtained results are also transferred in MATLAB using a high speed serial monitor of the DSP card. A block diagram of rapid prototyping control is shown in figure 5.

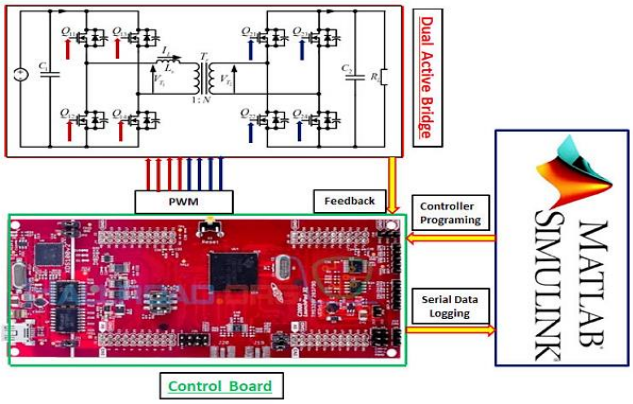

Figure 5 Rapid prototyping using DSP control card and MATLAB

A. *Voltage regulation with conventional control*

The experimental results collected using high speed serial monitor of the DSP card for the voltage regulation experiment of bidirectional dual active bridge with conventional PI controller and with varying input signal are presented in in Figure 6 and figure 7 respectively. The input command is varied between 24 and 14 volts at t=80 *ms* and set to 24 V at t =250 *ms*. During the first transition; the controller tracks it reference very slowly with a measured settling time (Ts) of 115 *ms*. However, the rising interval (Tr) of the system is 21.5 *ms*. In addition, the overall tracking response of the controller is very slow due to nonlinear behaviour of DAB. The variations in angle phi with respect to the input command are shown in Fig. 7. The phase shift of PWM register count of the DSP card is in the range selected from 0 and 250 counts which correspond to 0° and 90° respectively. The experimental voltage response is shown in Fig. 8 and it is similar to the voltage response of figure 6 recorded via high speed serial monitor.

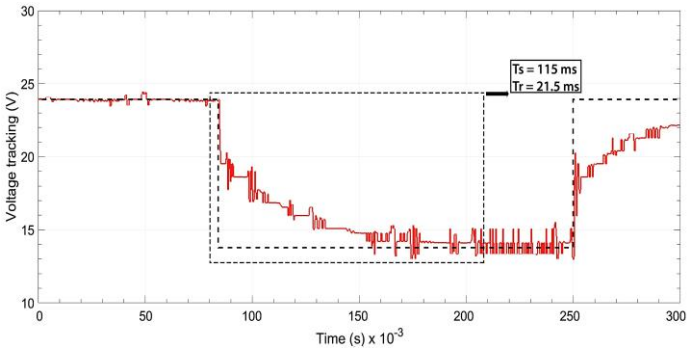

Figure 6. Voltage response of PI controller for variable reference command

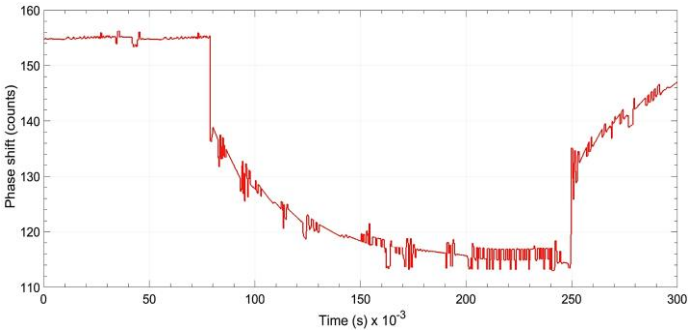

Figure 7 Phase shift using of PI controller under variable reference command

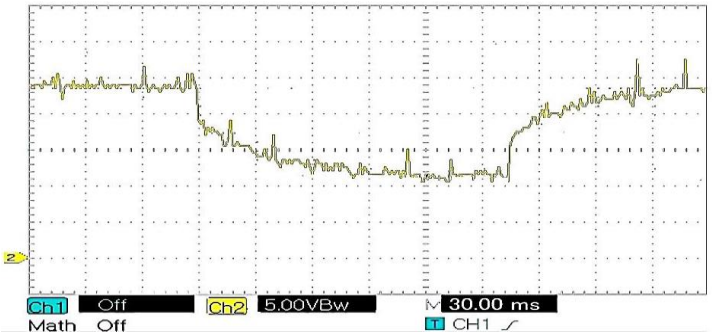

Figure 8 Experimental voltage responses with PI controller for variable reference command

B. *Voltage regulation with proposed control scheme*

The results for voltage regulation experiment of bidirectional dual active bridge with proposed controller and with varying input signal are presented in in Fig. 9, 10 and 11. With the proposed control, the steady state error in voltage tracking signal is close to zero while from the previous experimental results, it is concluded that the system shows large steady state error with the conventional PI control. From the presented results, measured settling time Ts is noted as 0.6 *ms* and rise time is 0.02 *ms*, which depicts the superior performance of the system under the action of proposed control system. From Fig. 9, at t = 250 i, a steady state error of 2.5 v and -1.5 v are observed for a short time of interval. In addition, with the proposed controller, the corresponding phase shift adjusts itself in finite time while tracking its reference and it is shown in Fig. 10.

The experimental voltage response with FO-PI controller is shown in Fig. 11 and it is similar to the voltage response of figure 9 recorded via high speed serial monitor

International Journal of Engineering Research & Technology (IJERT)
ISSN: 2278-0181
Vol. 11 Issue 04, April-2022

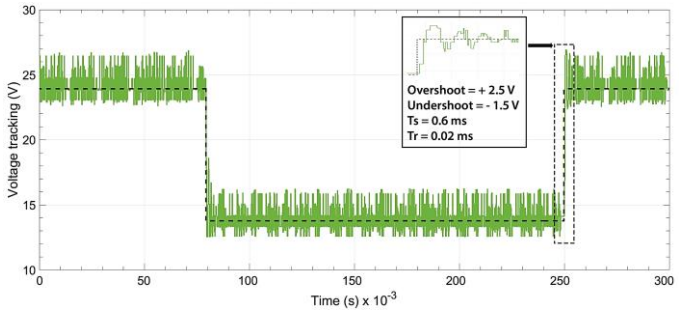

Figure 9 Voltage response of PI controller for variable reference command

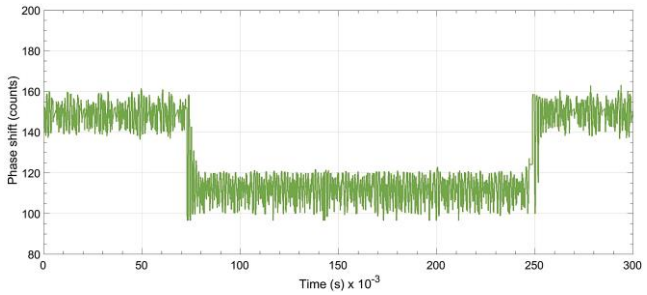

Figure 10 Phase shift using of PI controller under variable reference command

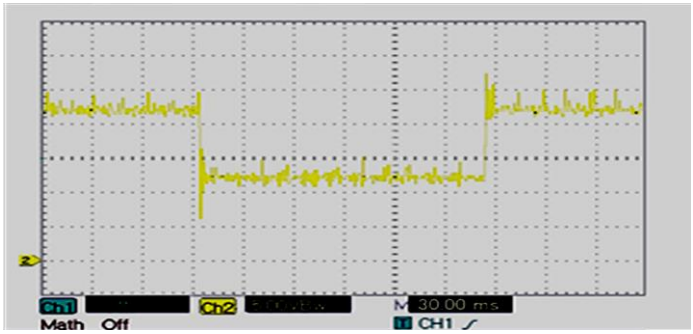

\

Figure 11 Experimental voltage responses with FO-PI controller for variable reference command

IV. CONCLUSIONS AND FUTURE RECOMMENDATION

This paper analyzed the stability and robustness of FO-PI controller for a micro-grid integrated bi-directional DAB utilized for battery storage system. On this basis, the proposed FO-PI controller is tested experimentally using a Texas Instrument DSP control card and a laboratory scaled DAB test bench. The collected experimental results for the proposed control is compared to the conventional PI controller and it is concluded that under variable reference command , the proposed controller outperforms the conventional PI controller in terms of rise time, settling time and steady state error. However the fractional order PI controller introduced high frequency noise in the tracking and control signals. Future recommendations include the tuning of filter parameter for the implementation of fractional operator for the elimination of noise.

REFERENCES

[1] Z. Farooq, T. Zaman, M. A. Khan, Nasimullah, S. M. Muyeen and A. Ibeas, "Artificial Neural Network Based Adaptive Control of Single Phase Dual Active Bridge With Finite Time Disturbance Compensation," in IEEE Access, vol. 7, pp. 112229-112239, 2019.

[2] K. Shen et al., "ZVS Control strategy of dual active bridge DC/DC converter with triple-phase-shift modulation considering RMS current optimization," in The Journal of Engineering, vol. 2019, no. 18, pp. 4708-4712, 7 2019.

[3] M. I. Rahman, K. H. Ahmed and D. Jovcic, "Analysis of DC Fault for Dual-Active Bridge DC/DC Converter Including Prototype Verification," in IEEE Journal of Emerging and Selected Topics in Power Electronics, vol. 7, no. 2, pp. 1107-1115, June 2019.

[4] B. Gu, J.-S. Lai, N. Kees, C. Zheng, Hybrid-switching full-bridge dc-dc converter with minimal voltage stress of bridge rectifier, reduced circulating losses, and filter requirement for electric vehicle battery chargers, IEEE Trans. Power Electron, 28(3), 1132-1144, 2013.

[5] Y. Shi, R. Li, Y. Xue, and H. Li, Optimized operation of current-fed dual active bridge DC-DC converter for PV applications, IEEE Trans. Ind. Electron,62(11),6986-6995, 2015.

[6] H. Tao, A. Kotsopoulos, J. L. Duarte, and M. A. M. Hendrix, Multi input bidirectional dc-dc converter combining dc-link and magnetic coupling for fuel cell systems, in Proc. 40th IEEE IAS Annu. Meeting, 3, 2021-2028, 2005.

[7] C.-C. Hua, Chih-Wei Chuang, Chun-Wei Wu, and Deng-Jie Chuang, Design and implementation of a digital high-performance photovoltaic lighting system, in Proc. ICIEA, pp. 2583-2588,2007.

[8] H. Bai, and C. Mi, Eliminate reactive power and increase system efficiency of isolated bidirectional dual-active-bridge dc-dc converters using novel dual-phase-shift control, IEEE Trans. Power Electron, 23(6), 2905-2914, 2008.

[9] Zhao Biao,Yu Qingguang,Sun Weixin Bi-directional Full bridge DC-DC Converters with Dual-phase-shifting Control and Its Backflow Power Characteristic Analysis, Proceedings of the CSEE, 32(012). 2012.

[10] Y. A. Harrye, K. H. Ahmed, G. P. Adam and A. A. Aboushady, "Comprehensive steady state analysis of bidirectional dual active bridge DC/DC converter using triple phase shift control, in 2014 IEEE 23rd International Symposium on Industrial Electronics (ISIE), 437-442, 2014.

[11] K. J.Astrom and T. H agglund, PID Controllers: Theory, Design, and Tuning. Research Triangle Park, NC: Instrument Society of America, 1995.

[12] J.-B. He, Q.-G. Wang and T.-H. Lee, PI/PID controller tuning via LQR approach, Chemical Engineering Science, 55(13), 2429 - 2439, 2000.

[13] S.Sumathi, Bansilal, Artificial Neural Network Application for Voltage Control and Power Flow control in Power Systems with UPFC, inproc. IEEE International conf. Emerging Research in Electronics, Computer Science and Technology, 2015.

[14] N. Ullah, M. Asghar Ali, A. Ibeas and J. Herrera, Adaptive Fractional Order Terminal Sliding Mode Control of a Doubly Fed Induction Generator-Based Wind Energy System, in IEEE Access, 5, 21368-21381, 2017.

[15] N. Ullah, M. A. Ali, R. Ahmad, and A. Khattak, Fractional order control of static series synchronous compensator with parametric uncertainty, IET Generat., Transmiss. Distrib, 11(1), 289-302, 2017.

[16] Ullah, N., Khattak, M.I., Khan, W, Fractional order fuzzy terminal sliding mode control of aerodynamics load simulator, Proc. Inst. Mech. Eng., Part G: J. Aerospace Eng. 229 (14), 2608-2619, 2015.

[17] F. Zhang and C. Li, Stability analysis of fractional differential systems with order lying in, Advances in Difference Equations. 2011(/2011) 213485.

[18] C. Li and W. Deng, Remarks on fractional derivatives, Applied Mathematics Computation, 187(2007) 777-784